ANALYSIS OF FLOW IN CHANNELS WITH BOTTOM INTAKES

Adel Yassa

A Dissertation
in
The Faculty
of
Engineering

Presented in Partial Fulfillment of the Requirements
for the Degree of Master of Engineering at
Concordia University
Montreal, Quebec, Canada

May, 1979

CONCORDIA UNIVERSITY

ABSTRACT

ANALYSIS OF FLOW IN CHANNELS WITH BOTTOM INTAKES

by

Adel Yassa

Spatially varied flow equations are critically reviewed and the inconsistencies existing in their derivations are brought out. The historical development of the analysis of flow through bottom intakes which represent a special case of steady spatially varied flow is traced.

An analytical expression for the entrance depth of a slot at the bed of a horizontal channel is derived in terms of the slot length, the Froude number of the approach flow and the performance factor; the expression was verified for supercritical flow.

Experimental data on bottom racks with bars transverse to the flow direction and racks with small orifices or perforations are analyzed using Mostkow's equations. The coefficients of discharge are computed and their behaviour is discussed. The flow profiles predicted by Mostkow's equations are in satisfactory agreement with the observed profiles.

ACKNOWLEDGEMENTS

The author wishes to express his gratitude to his supervisors, Dr. A. S. Ramamurthy and Dr. M. S. Nasser, for suggesting the topic and for their sustained encouragement.

The author also expresses his profound thanks to Dr. P. Venkataraman for his continuous help during the preparation of this work.

Appreciation is also extended to Mrs. Julie Strick for typing this dissertation.

Montreal, Quebec
May 1979

Adel Yassa

TABLE OF CONTENTS

LIST OF TABLES

LIST OF FIGURES

NOMENCLATURE

SYMBOL		DESCRIPTION
A	-	Area of water flow
B	-	Width of bottom rack or channel
C_1	-	Coefficient of discharge for rack with parallel bars
C_2	-	Coefficient of discharge for rack with orifices
D	-	Hydraulic depth
E	-	Specific energy
F	-	Froude number
F_o	-	Froude number of incoming flow
g	-	Acceleration due to gravity
L, ℓ	-	Total length of rack
$\delta\ell$	-	Spacing of rack
ΔM	-	Change in momentum
P	-	Resultant pressure
Q, Q_o	-	Incoming discharge
Q_d	-	Diverted discharge
Q_R	-	Residual discharge
q_o	-	Incoming discharge per unit width of channel
S_e	-	Energy slope
S_o	-	Bed slope

SYMBOL		DESCRIPTION
S_f	-	Friction slope
T	-	Top width of flow
V, V_o	-	Velocity of incoming flow
V_d	-	Velocity of diverted flow
x	-	Distance along the rack from the upstream end
Y_o, y_o	-	Depth of the incoming flow
Y_R	-	Depth of the residual flow
y	-	Depth of flow at a section in the rack
y_1	-	Depth of flow at the upstream end of the rack
y_2	-	Depth of flow at the downstream end of the rack
α	-	Energy coefficient
ϕ	-	Angle made by the velocity vector of diverted flow with the channel bed
η	-	Performance factor, ratio of diverted flow to main flow
ζ_1	-	Pressure correction factor at upstream end of rack
ζ_2	-	Pressure correction factor at downstream end of rack
γ	-	Specific weight of water
ε	-	Ratio of the area of openings to the total area of rack (opening area ratio)

CHAPTER 1

INTRODUCTION

Spatially varied flow is encountered in an open channel which has a nonuniform discharge resulting from the addition or diminution of water along the flow direction. This type of flow is found in side-channel spillways, side-weirs, roadside gutters, washwater troughs in filters, effluent channels around sewage-treatment tanks, and the main drainage channels and feeding channels in irrigation systems [8]. The dynamic equations describing the water surface profiles in a channel with spatially varied flow are analyzed in various forms to cover a multitude of practical applications. In reviewing the literature, several inconsistencies have been detected among these expressions.

Flow in a channel with a bottom rack represents a case of spatially varied flow. Scanning through the literature available on flow through bottom racks, one finds that the constant energy assumption conventionally employed in previous works requires re-examination. Further, the extent of influence of the state of approach flow on the coefficient of discharge is not properly evaluated.

This study presents an attempt to determine the effect of Froude number on the discharge coefficient utilizing Venkataraman's data [15]. The theoretical analysis is simplified by considering different sizes of

rectangular bed-slots, spanning the entire width of the channel; the appropriate momentum equation is applied in a direction normal to the direction of flow. An expression for the ratio of the depth at the beginning of the opening to its length, is obtained and is verified on the basis of the reported data in ref. 15. In addition, the flow profiles have been obtained using Mostkow's equations [9] for racks with bars perpendicular to the direction of flow and for racks with small orifices; these are then compared with Venkataraman's experimental profiles [15].

In order to furnish a basis for understanding the problem, Chapter 2 presents a review of the governing equations and the state of the art on flow behaviour in channels with bottom racks.

The theoretical analysis and experimental verification are presented in detail in Chapter 3.

Chapter 4 summarizes the important findings of this study and suggests possible areas where further work can be carried out.

CHAPTER 2

REVIEW OF LITERATURE

2.1 GENERAL REMARKS

The review presented in this chapter deals with two aspects of the phenomenon under study. In the first section, the dynamic equations describing the spatially varied flow with either increasing or decreasing discharge are discussed with an emphasis on certain discrepancies that exist among them. The available literature on flow through bottom racks is briefly described in a later stage in order to illustrate the method of attack employed in the present study.

2.2 REVIEW OF SPATIALLY VARIED FLOW EQUATIONS

Conservation of mass in conjunction with either the momentum principle or the energy principle are generally used in the derivation of spatially varied flow equations. Because of the basic difference in the physical concept between the momentum and the energy principles, the expressions obtained based on either approach will be inherently different. The momentum approach is a vector relationship which equates the net momentum flux to the external forces acting on a control volume in the direction of flow, while the energy approach is a scalar relationship considering

the work done by the gravity force and the energy dissipation due to internal stresses within the control volume.

Numerous investigations have been carried out on the theoretical and the experimental aspects of spatially varied flow in open channels [1,3,4,5,7,8,10,17]. The majority of these studies treat both the cases of increasing and decreasing discharge [3,4,5,10,17]; refs. [1,7] relate to flow with decreasing discharge and ref. [8] solely describes the flow with increasing discharge.

Recently more studies have been directed to derive generalized spatially varied flow equations for increasing as well as decreasing discharges [5,17].

The general assumptions made in the derivation of the spatially varied flow equation may be summarized as follows [4]:

1. The flow is unidirectional
2. The velocity distribution across the channel section is constant and uniform
3. The pressure in the flow is hydrostatic
4. The slope of the channel is relatively small
5. The Manning formula is used to evaluate the friction loss
6. The effect of air entrainment is neglected.

Hinds [8] was one of the earliest investigators to carry out a theoretical analysis of the problem of spatially varied flow with increasing discharge. Using the momentum principle, he derived a flow profile, applicable to channels of any shape. The momentum of the lateral inflow in the channel was not considered as the inflow was assumed to enter the

main channel at right angles and the frictional resistance was neglected. Hinds' equation at two consecutive sections separated by a small finite distance Δx is:

$$\frac{\Delta y}{\Delta x} = \frac{Q}{g}\left(\frac{V + \frac{1}{2}\Delta v}{Q + \frac{1}{2}\Delta Q}\right)\left[\frac{\Delta v}{\Delta x} + \frac{v}{Q}(v + \Delta v)\right] \quad \ldots\ldots\ldots\ldots (2.1)$$

where —

Q = the discharge in cubic feet per second

g = acceleration due to gravity

v = velocity in feet per second

y = head of water

$\frac{\Delta y}{\Delta x}$ = water-surface slope

Nimmo [10] derived two equations, one for spatially varied flow with increasing discharge and the other for decreasing discharge, using the momentum approach. His equations, simplified for a rectangular prismatic channel, take the forms:

$$\frac{dy}{dx} = \frac{S_o - S_f - 2Qq_o/gA^2}{1 - Q^2/gA^2y} \quad \text{— (for increasing discharge)} \ldots (2.2a)$$

$$\frac{dy}{dx} = \frac{S_o - S_f - Qq_o/gA^2}{1 - Q^2/gA^2y} \quad \text{— (for decreasing discharge)} \ldots\ldots (2.2b)$$

where —

q_o = the incoming discharge per unit width of channel

S_o = bed slope

S_f = friction slope

A = area of water flow.

It can be seen that the difference in these two equations lies only in the coefficient of the third term in the numerator on the right hand side.

De Marchi [7] carried out analytical and experimental investigations on the flow of water over side-weirs assuming the energy head along the weir crest to be constant. He concluded that the water surface profile over the weir is essentially curved (rising in subcritical flow and dropping in supercritical flow). De Marchi's equation is identical to that proposed by Nimmo. For horizontal channels, the flow profile is given by:

$$\frac{dy}{dx} = \frac{-Qq_o/gA^2}{1-Q^2/gA^2y} \qquad \ldots\ldots\ldots (2.3)$$

The two equations obtained by Chow [3] are:

$$\frac{dy}{dx} = \frac{S_o - S - 2\alpha Qq_o/gA^2}{1 - \alpha Q^2/gA^2D} \quad \text{(for increasing discharge)} \ldots\ldots (2.4a)$$

$$\frac{dy}{dx} = \frac{S_o - S - \alpha Qq_o/gA^2}{1 - \alpha Q^2/gA^2D} \quad \text{(for decreasing discharge)} \ldots\ldots (2.4b)$$

where —

D = hydraulic depth = $\frac{\text{Flow area, } A}{\text{Top Width, } T}$

α = energy coefficient

He indicated that the momentum principle or the energy principle could be applied to obtain these equations. However, he favours the use of the energy equation for the case of lateral outflow. Such a preference is not justified, since both approaches stem from Newton's second law; thus when applied to any open channel flow phenomenon should lead to identical results. Further, Chow does not consider the sense of the flow,

i.e., accroding to his equations, inflow or outflow would have the same influence on the flow profile. It might have been more logical and general to obtain identical equations to describe both types of flow and assign a positive sign to take care of the case with inflow and a negative sign for the outflow case. Also, the occurrence of the coefficient 2 in the third term of the numerator describing the lateral flow is not explained adequately.

In a later study, Chow obtains equations for the slope of the water surface for flow with increasing discharge using the momentum approach and uses the energy principle for flow with decreasing discharge [4]. The two new equations are identical to the earlier ones [3].

It should be noted that these equations are applicable only for some cases of flow and cannot be universally employed.

Then Chow [5] proceeds to establish that both the momentum and the energy principles are equally applicable in the derivation of the spatially varied flow equations and derives identical equations for either increasing or decreasing discharge, viz.

Equations based on momentum principle (for $U \cos\phi = 0$):

$$\frac{dy}{dx} = \frac{S_o - S_f - 2Qq_o/gA^2}{1 - Q^2/gA^2y} \quad \text{(for increasing discharge)} \quad \ldots (2.5a)$$

$$\frac{dy}{dx} = \frac{S_o - S_f - 2Qq_o/gA^2}{1 - Q^2/gA^2y} \quad \text{(for decreasing discharge)} \quad \ldots (2.5b)$$

Equations based on Energy principle (for $V = U = U \cos \phi$):

$$\frac{dy}{dx} = \frac{S_o - S_e - Qq_o/gA^2}{1 - Q^2/gA^2y} \quad \text{(for increasing discharge)} \quad \ldots\ldots (2.5c)$$

$$\frac{dy}{dx} = \frac{S_o - S_e - Qq_o/gA^2}{1 - Q^2/gA^2y} \quad \text{(for decreasing discharge)} \quad \ldots\ldots (2.5d)$$

This cannot be true because the equations would yield identical profiles whether the flow is an inflow or outflow.

Yen and Wenzel [17] performed a theoretical analysis using both momentum and energy principles for the case of steady flow of an incompressible viscous fluid in a prismatic channel with spatially variable lateral inflow or outflow. They considered the sense of the lateral flow, an aspect that was neglected by all earlier investigators. They obtained generalized equations for flow profiles that would be applicable for both the outflow and inflow case and assigned a positive sign for the inflow and a negative sign for the outflow. Their simplified equations are:

Based on Momentum principle:

$$\frac{dy}{dx} = \frac{S_o - S_f + (q_o/gA)(U\cos\phi - 2V)}{1 - Q^2/gA^2y} \quad \text{(for increasing discharge)} \ldots (2.6a)$$

$$\frac{dy}{dx} = \frac{S_o - S_f - (q_o/gA)(U\cos\phi - 2V)}{1 - Q^2/gA^2y} \quad \text{(for decreasing discharge)} \ldots (2.6b)$$

Based on Energy principle:

$$\frac{dy}{dx} = \frac{S_o - S_e + (q_o/2gAV)(U^2-3V^2)}{1 - Q^2/gA^2y} \quad \text{(for increasing discharge)..... (2.6c)}$$

$$\frac{dy}{dx} = \frac{S_o - S_e - (q_o/2gAV)(U^2-3V^2)}{1 - Q^2/gA^2y} \quad \text{(for decreasing discharge)..... (2.6d)}$$

These equations lack experimental verification; it is difficult, therefore, to evaluate their validity for practical cases.

It is noted that Yen and Wenzel's Eq. (2.6a) is the same as Eq. (2.4a) obtained by Chow for lateral inflow at right angles, but Eq. (2.6b) differs from Chow's Eq. (2.4b). On the other hand their Eq. (2.6c) is different from Chow's Eq. (2.4a), while their Eq. (2.6d) is identical with that of Chow Eq. (2.4b).

El-Khashab and Smith [1] carried out analytical and experimental investigations of flow over side weirs and concluded that the traditional assumption of constant total energy in the side-weir channel has not been substantiated. For decreaseing discharge they employ the energy principle and their equation for the slope of the water surface is the same as that of Chow Eq. (2.4b). Their equation obtained from the momentum principle is the same as that of Yen and Wenzel (Eq. 2.6b).

El-Khashab and Smith's equations for the two cases are:

Momentum Principle:
$$\frac{dy}{dx} = \frac{S_o - S_f + q_o/gA\ (2V-U\cos\phi)}{1 - Q^2/gA^2y} \quad \ldots\ldots\ldots \text{(2.7a)}$$

Energy Principle:
$$\frac{dy}{dx} = \frac{S_o - S_e - q_o/2gAV\cdot(U^2-3V^2)}{1 - Q^2/gA^2y} \quad \ldots\ldots\ldots\ldots \text{(2.7b)}$$

2.3 Review of Flow in Channels with Bottom Racks

The bottom intake or bottom rack represents a simple hydraulic device used to divert the flow in an open channel. This device consists of a rack composed of bars arranged to form a grid structure. The bars of grid may be either parallel to the direction of flow or transverse to it. Alternatively, this device may be made up of perforated screens (see Fig. 1).

Flow in a channel with bottom intakes represents a case of spatially varied flow with decreasing discharge (Fig. 2). Bottom intakes have a number of applications such as: [14]

1. In a large canal system where flow in excess of that required in the main canal may be diverted to some convenient location
2. As horizontal trash racks in the hydro-power plants located on mountain streams
3. In the sedimentation tanks to trap the debris in the grit chambers
4. As kerb-outlets on the side of main streets to drain storm waters into the subsurface drains
5. As skimmers when it is desired to reduce the volume of water to transport fish.

Determining the performance of a bottom rack is a complex problem due to the large number of variables involved. Many investigations have been carried out to effect a proper design for a bottom intake and to analyze the phenomenon of flow through it.

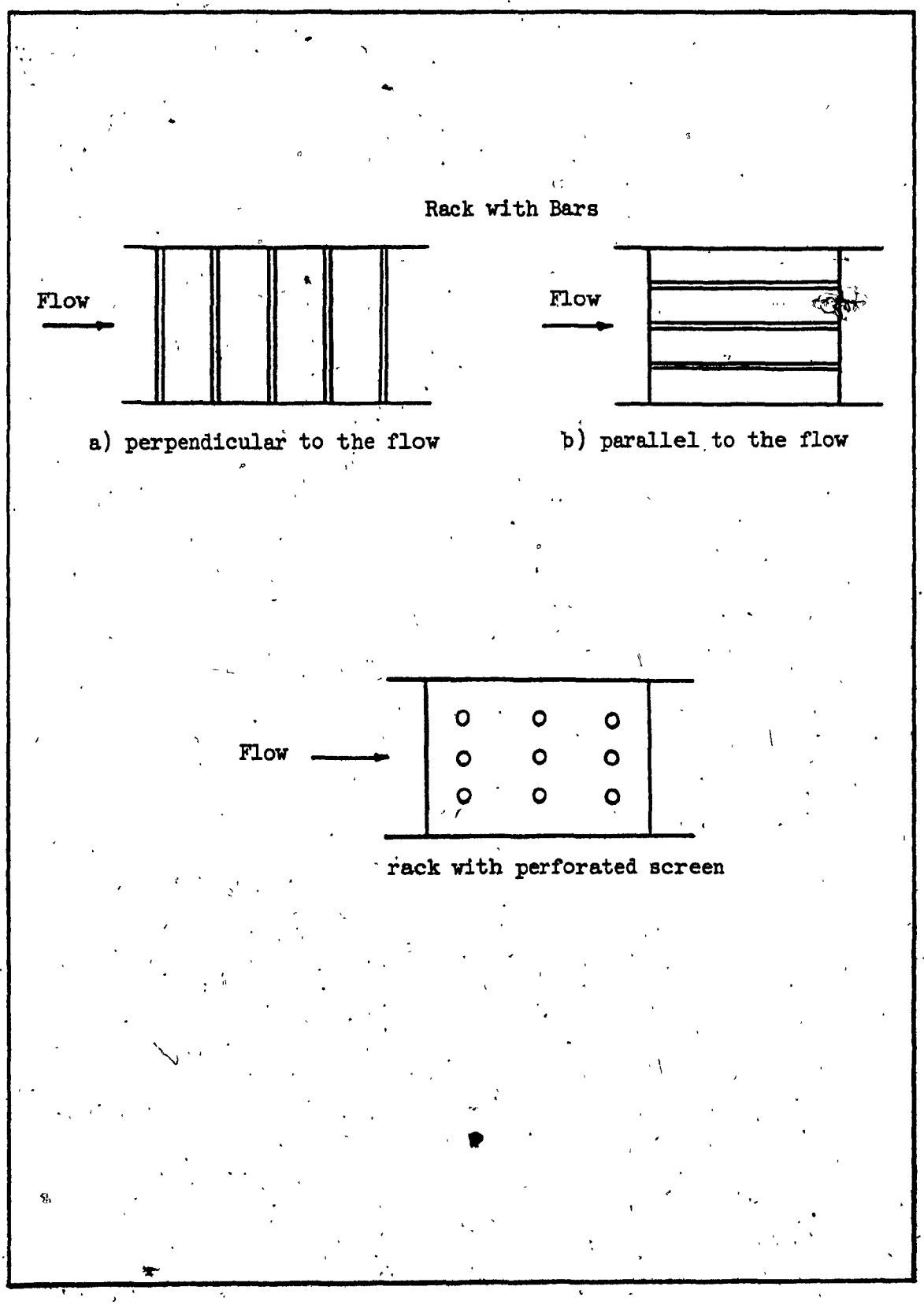

Fig. 1 — Types of Racks.

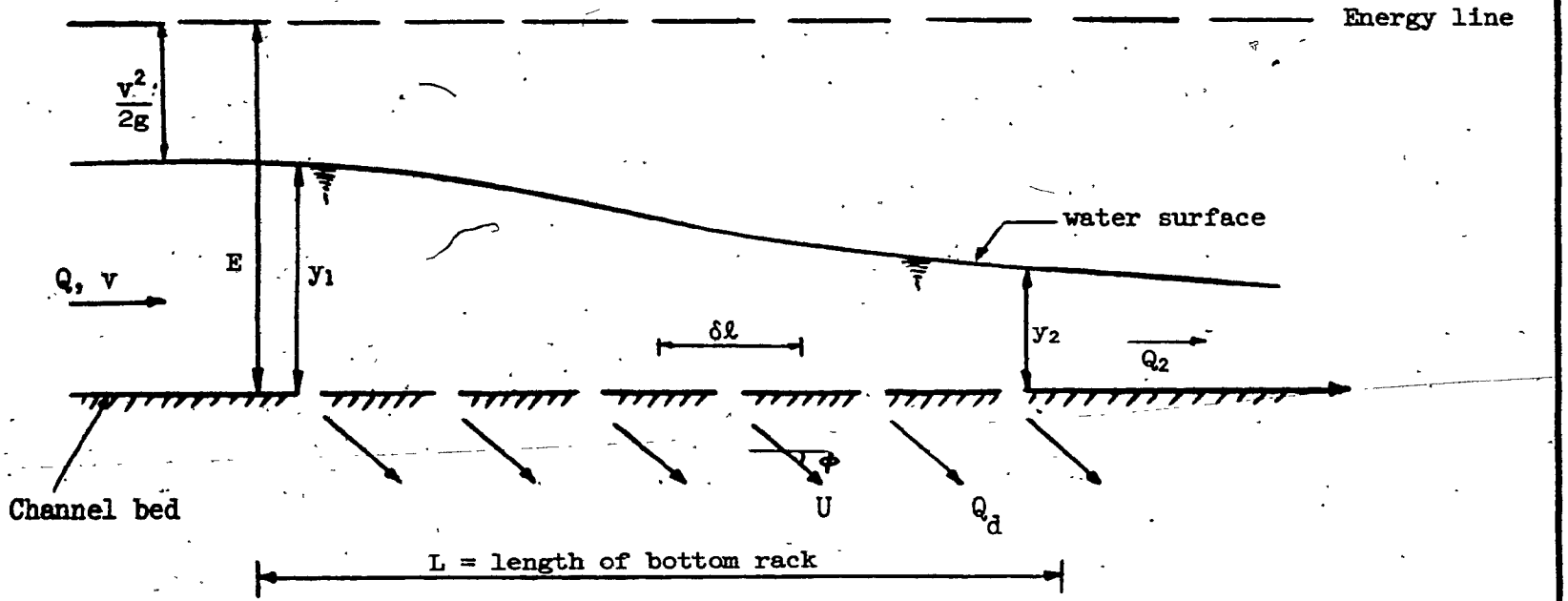

$\delta\ell$ = spacing of racks

Q = discharge at a section in the channel

Q_d = lateral outflow per unit length of the channel.

Fig. 2 — Definition Sketch (spatially varied flow).

Bovard [2] proposed that the diverted flow depends upon the depth of flow over the rack. He obtained a 1st order differential equation with six variables for the rate of diverted flow through the rack. However, the results of his experiments on transverse racks did not conform to his theoretical analysis.

Orth, Chardonnet and Meynardi [12] carried out different model tests on intakes of varying lengths having rack bars of different shapes. From experiments they found the best hydraulic performance was attained with rack-bars of oval cross-section which permitted flushing of all sizes of gravel and maintained the desired flow through the rack bars. The bars were oriented transverse to the flow.

Noseda [11] carried out his experiments on different bar sizes. In the majority of cases the bars were parallel to the direction of flow; the flow surface profiles were recorded. Noseda assumed constant specific energy and obtained, analytically, the characteristics of an ideal bottom intake. He noticed that the coefficient of discharge decreased as the ratio of the area of the openings to the total area increased.

Mostkow [9] proposed, perhaps the most generally accepted analysis. His experiments were conducted on intakes having transverse bars and perforations. He considered that the specific energy along the channel remained constant. He, further, noticed that when the direction of flow through the rack openings is nearly vertical, the energy loss is negligible and in this case the effective head on the rack is practically equal to the specific energy. Mostkow found that this is true for racks with parallel bars. When the direction of flow through the rack openings makes an appreciable angle with the vertical, it results in a loss of energy; this

is because the flow impinges on the sides of the openings, and a change in the direction of flow from inclined to vertical will occur eventually. This was confirmed experimentally for racks with perforated screens.

For flow through racks with parallel bars where the flow is vertical, Mostkow proposed the following formula:

$$x = \frac{E}{\varepsilon C_1}\left(\frac{y_1}{E}\sqrt{1 - \frac{y_1}{E}} - \frac{y}{E}\sqrt{1 - \frac{y}{E}} \right) \qquad \ldots\ldots\ldots\ldots (2.8a)$$

and for inclined flow through racks with perforated screens:

$$x = \frac{E}{\varepsilon C_2}\left[\frac{1}{2}\cos^{-1}\sqrt{\frac{y}{E}} - \frac{3}{2}\sqrt{\frac{y}{E}\left(1-\frac{y}{E}\right)} - \frac{1}{2}\cos^{-1}\sqrt{\frac{y_1}{E}} + \frac{3}{2}\sqrt{\frac{y_1}{E}\left(1 - \frac{y_1}{E}\right)} \right]$$

$$\ldots\ldots\ldots\ldots (2.8b)$$

where —

x = the distance along the rack from its upstream end

E = specific energy at the section

ε = ratio of the area of the openings to the total area of rack (opening area ratio)

C_1, C_2 = coefficient of discharge through the openings

y_1 = depth of flow at the upstream end of the rack

y = depth of flow at a section in the rack.

The value of the coefficients of discharge, through the rack openings actually varies considerably along the rack. In general, he found that these coefficients are higher for racks with perforated screens than for racks with parallel bars. The value is higher for horizontal racks than for inclined racks.

Drimmer [6] obtained a differential equation of the first order with five variables to analyze the shape of the nappe in the case of steady flow, over a bottom intake with rack-bars oriented along the flow.

2.4 Concluding Remarks

From the preceding presentation, it is seen that there is a need for the revision of the spatially varied flow equations, since the derived equations by most of the investigators are contradictory. Also, each equation is applicable only for some cases of flow and cannot be generalized.

From the point of view of practical application, it is seen that in general, the energy equation is preferred for spatially varied flow with decreasing discharge and the momentum equation is preferred for increasing discharge, although such a preference is unnecessary.

The review of flow in channel with bottom racks, demonstrates that each investigation is valid only for the conditions under which it was conducted. A generalized theory is not yet available.

CHAPTER 3

ANALYSIS

3.1 GENERAL REMARKS

The brief survey of literature on analysis of flow in channels with bottom rack reveals that most of the existing studies are based either on empirical assumptions or assumptions that are challenged by recent investigators. It is believed that the study of a channel with a slot at its bed, spanning its entire width [Fig. 3] would provide a better understanding of the flow behaviour. Since there are no rack bars, the area factor ε, defined as the ratio of the area of the openings to the total area of rack is unity. The flow is two-dimensional; the assumption that the energy correction factor, α, and the momentum factor, β, is equal to unity would further simplify the problem to a one-dimensional case. The slot then represents a simplified bottom rack and is easily amenable to theoretical analysis. Further, the findings of such an analysis could be easily extended to the case of flow through a bottom rack, and might form a rational basis for the evolution of a proper design procedure for bottom racks.

3.2 THEORETICAL ANALYSIS OF FLOW THROUGH BOTTOM SLOTS

By applying the momentum equation in a direction parallel to the channel bed, (Fig. 3), Venkataraman [13] has obtained an equation relating

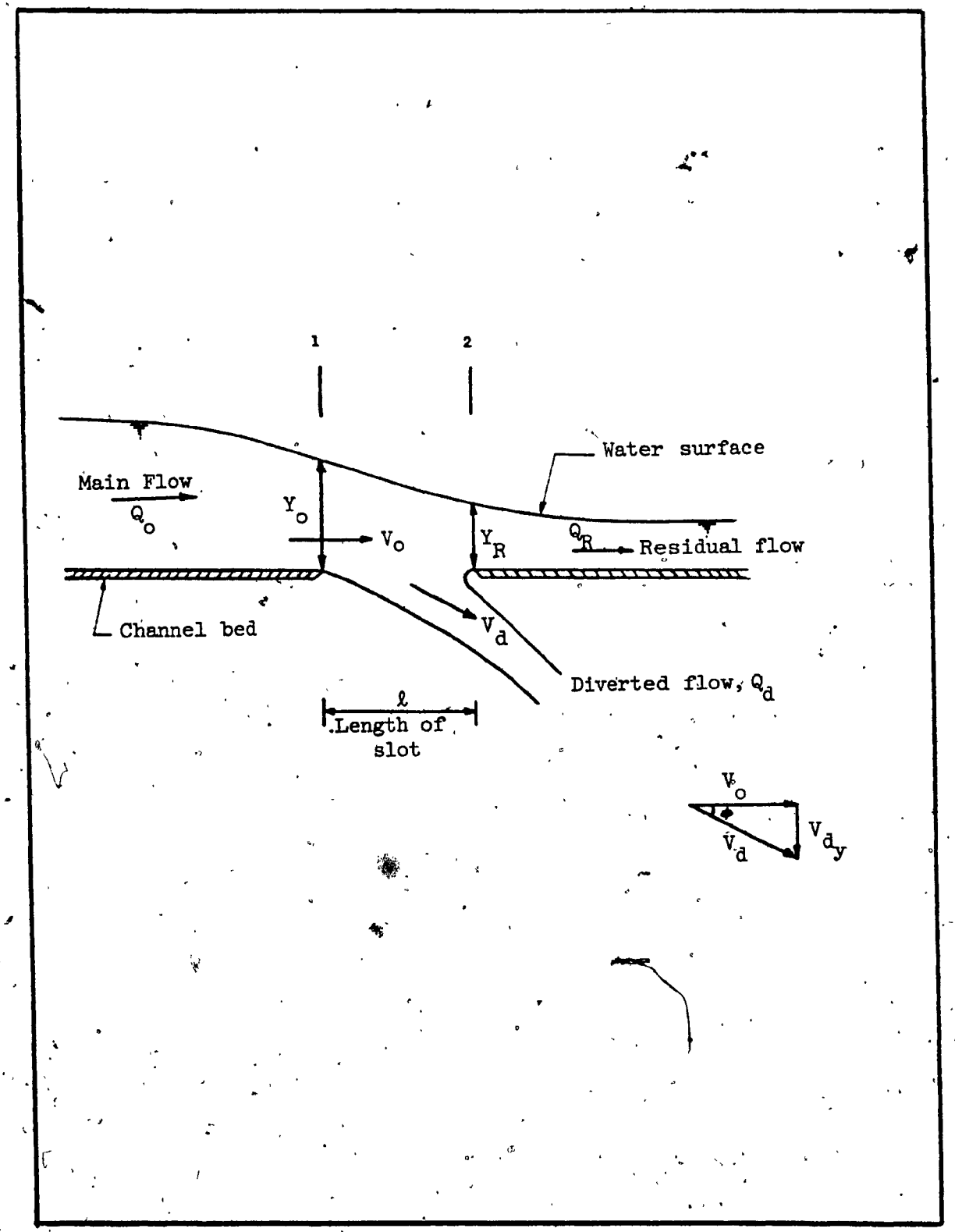

Fig. 3 — Definition Sketch (Bottom slot).

the flow depths at the upstream and the downstream ends of the openings.

$$\zeta_2 \left[\frac{Y_R}{Y_o}\right]^3 + \left[F_o^2 \eta - F_o^2 - \zeta_1\right] \frac{Y_R}{Y_o} + F_o^2 [1 - \eta]^2 = 0 \quad \ldots\ldots (3.1)$$

where —

Y_o, Y_R = the flow depths at the beginning and end of the slot of length ℓ

F_o = Froud number of the incoming flow = $\left[\frac{q_o^2}{gy_o^3}\right]^{1/2}$

η = performance factor, defined as the ratio of the diverted discharge, Q_d, to the channel main flow, Q_o

ζ_1 and ζ_2 = pressure correction factors and varies with the flow curvature at the section

If the streamlines were parallel to the channel bed, the pressure distribution at any section would be hydrostatic. Then, the pressure correction factor is defined by

$$P = \zeta \cdot \gamma \cdot h^2 \quad \ldots\ldots\ldots (3.2)$$

where —

P = resultant pressure at the section and $\zeta = 0.50$.

Therefore, when hydrostatic pressure distribution prevails at sections 1 and 2, $\zeta_1 = \zeta_2 = 0.50$. Eq. (3.1) reduces to a three variable expression. For this case, the solutions of the equation were represented in the form of a chart relating $\frac{Y_R}{Y_o}$ to F_o for different values of η [15].

It is felt that it is more logical to relate Y_o/ℓ, F_o, and η instead of Y_R/Y_o, F_o and η. The flow conditions can then be described in terms of the upstream depth and slot length only and the influences of slot

length on flow parameters could be evaluated.

In order to obtain an expression for Y_o/ℓ, the momentum change of the water body above the opening is now resolved in the vertical direction and equated to the external forces in the same direction. The change in momentum, ΔM, in the vertical direction is affected only by the vertical component of the diverted flow. Therefore:

$$\Delta M = \frac{\gamma Q_d}{g} \cdot V_{d_y} \qquad \ldots\ldots\ldots\ldots\ldots\ldots \quad (3.3)$$

where —

γ = specific weight of water

Q_d = diverted flow quantity

g = acceleration of gravity

V_{d_y} = the diverted flow velocity in the y-direction.

The component of the diverted velocity, V_d, in the direction of flow may be assumed to be equal to the velocity, V_o of the channel flow at the section where lateral flow leaves the main flow, i.e.,

$$V_o = V_d \cos \phi \qquad \ldots\ldots\ldots\ldots\ldots\ldots \quad (3.4)$$

where —

ϕ = angle made by the velocity vector at the section, with the x-direction.

$$\text{Hence, } \tan \phi = \eta \cdot Y_{o/\ell} \qquad \ldots\ldots\ldots\ldots\ldots\ldots \quad (3.5)$$

The weight of water above the opening represents the only external force, P_v in the vertical direction, i.e.

$$P_v = \gamma \left(\frac{Y_R + Y_o}{2} \right) \cdot \ell \cdot B \qquad \ldots\ldots\ldots\ldots\ldots\ldots \quad (3.6)$$

where B = width of the channel.

From equations 3.3, 3.4, and 3.6, one obtains:

$$\frac{Y_R}{Y_o} = 2\eta^2 F_o^2 \left(\frac{Y_o}{\ell}\right)^2 - 1 \quad \ldots\ldots\ldots\ldots\ldots\ldots (3.7)$$

The advantage of Eq. (3.7) lies in the absence of pressure correction terms. Equation (3.1) is now employed to reduce one of the variables from Eq. (3.7) so that the results could be represented in the form of compact charts.

If the pressure distribution at sections 1 and 2 were to be hydrostatic, Eq. (3.1) reduces to:

$$\left[\frac{Y_R}{Y_o}\right]^3 + \frac{Y_R}{Y_o}\left[2F_o^2\eta - 2F_o^2 - 1\right] + 2F_o^2[1-\eta]^2 = 0 \quad \ldots\ldots (3.8)$$

The two positive solutions of Y_R/Y_o are then evaluated by solving the cubical Eq. (3.8) for different values of F_o and η. The negative values are ignored. Table 1 summarizes these values.

Each of the known values of F_o, η, and Y_R/Y_o are then substituted in Eq. (3.7) which is then solved to yield the positive and the negative root of Y_o/ℓ. The negative roots are neglected and the two positive solutions are related to the Froude number of the incoming flow with η as the third parameter in the charts presented in Fig. 4. These two depths are analogous, in a sense, to the sequent depths.

Table 2 summarizes the values of the positive roots of Y_o/ℓ for different values of F_o and η.

It is to be emphasized, at this point, that the charts represented by Fig. 4 have only limited application in view of the fact that they are based on the assumption that the pressure distributions at the

TABLE 1

VALUES OF Y_R/Y_0

F_0 \ η	0		0.2		0.4		0.6		0.8		1.0	
1	1.0	1.0	1.258	0.560	1.280	0.346	1.242	0.181	1.153	0.057	1.0	0.0
2	2.372	1.0	2.268	0.749	2.115	0.521	1.875	0.312	1.547	0.124	1.0	0.0
3	3.773	1.0	3.478	0.78	3.118	0.564	2.668	0.357	2.061	0.157	1.0	0.0
4	5.179	1.0	4.718	0.788	4.177	0.58	3.514	0.375	2.63	0.174	1.0	0.0
5	6.589	1.0	5.97	0.793	5.252	0.587	4.379	0.384	3.222	0.182	1.0	0.0

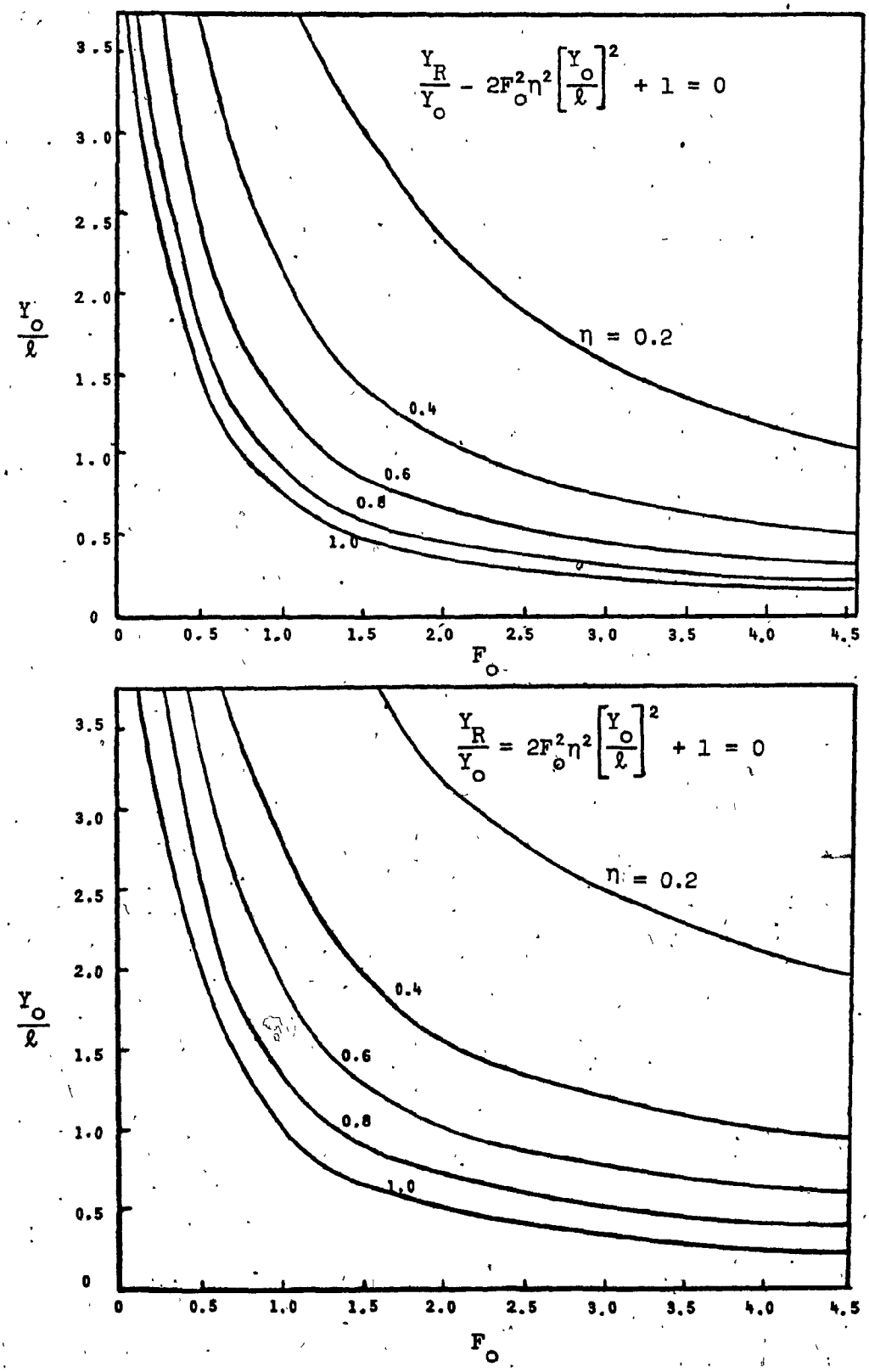

Fig. 4 — $\frac{Y_o}{\ell}$ as a function of F_o and η.

TABLE 2

VALUES OF Y_0/ℓ

F_o \ η	0		0.2		0.4		0.6		0.8		1.0	
1	∞	∞	5.31	3.90	2.67	2.05	1.77	1.28	1.30	0.91	1.0	0.71
2	∞	∞	3.20	2.34	1.56	1.09	1.0	0.68	0.71	0.47	0.50	0.35
3	∞	∞	2.49	1.57	1.20	0.74	0.75	0.46	0.52	0.32	0.33	0.24
4	∞	∞	2.11	1.18	1.01	0.56	0.63	0.35	0.42	0.24	0.25	0.18
5	∞	∞	1.87	0.95	0.88	0.45	0.55	0.28	0.36	0.19	0.20	0.14

beginning and the end of the opening are hydrostatic.

However, actual measurements [15,16] of the pressure distribution at the entrance and end of the opening have revealed that the pressure distribution is not hydrostatic. A typical pressure distribution for subcritical flow cases is presented in Ref. [16].

Fig. 5 discloses a typical pressure variation at the entrance and end of the opening of a supercritical flow case.

The pressure correction factors ζ_1 and ζ_2 are evaluated by integrating the pressure distribution profile using the Simpson rule, (Fig. 5).

The experimental data [15] for supercritical flow case are now inserted in conjunction with the computed pressure correction factors in Eq. (3.1) and the values of Y_R/Y_0 are obtained. These values are then substituted in Eq. (3.7) to get the values of Y_0/ℓ. Results of the computations are summarized in Table 3.

The computed values of Y_R/Y_0 and Y_0/ℓ are in reasonable agreement with the measured values.

3.3 Coefficient of Discharge of Bottom Racks

Experimental data for racks with narrow slits at right angles to the flow direction and for racks with perforated screens, were analyzed to get the flow profiles and the discharge coefficients. The analysis is based on the profile equations developed by Mostkow [9].

3.3.1 RACK WITH SLITS

For racks with parallel bars, Mostkow proposed the equation for flow profile, Eq. (2.8a) which is reproduced here for easy reference:

$\eta = 0.1543$ $F_o = 3.049$ $\ell/B = 3/30 = 0.10$.

UPSTREAM

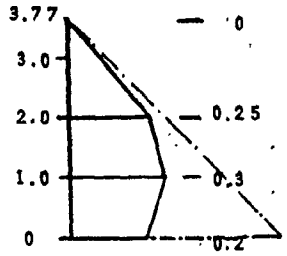

Area of pressure distribution curve using Simpson's rule

$= 0.771$

$= \zeta_1 \times 1 \times \overline{3.77^2}$

$\zeta_1 = 0.054$

DOWNSTREAM

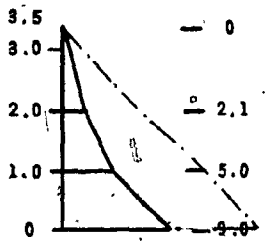

Area of pressure distribution curve using Simpson's rule

$= 11.785$

$= \zeta_2 \times 1 \times \overline{3.35^2}$

$\zeta_2 = 1.050$

—·—·— Hydraustatic pressure distribution.

Fig. 5 — Vertical pressure distribution at the beginning and end of the opening for a supercritical flow case.

TABLE 3

COMPARISON OF THEORETICAL AND EXPERIMENTAL VALUES OF Y_R/Y_o and Y_o/ℓ

Length of Slot, ℓ, cm	η (Q_o/Q_d)	Depths of Flow		F_o			Y_R/Y_o		Y_o/ℓ	
		Y_o cm	Y_R cm	$V_o/\sqrt{gY_o}$	ζ_1	ζ_2	From Expts.	From Eq. (3.1)	From Expts.	From Eq. (3.7)
3.0	0.1543	3.77	3.35	3.049	0.054	1.050	0.956	0.96	2.102	2.08
3.0	0.1612	3.57	3.37	3.103	0.032	0.861	0.9[illegible]	0.90	1.957	1.95
3.0	0.1961	3.53	3.36	2.699	0.074	0.926	0.913	0.82	1.848	1.80
3.0	0.2539	3.70	3.38	2.107	0.070	0.809	0.912	0.73	1.827	1.74
3.0	0.3493	3.68	2.90	1.673	0.04	0.644	0.846	0.62	1.644	1.54
4.0	0.1654	3.68	3.40	3.209	-0.028	1.114	0.948	0.99	1.859	1.88
4.0	0.1785	3.54	3.31	3.15	-0.005	0.998	0.916	0.94	1.741	1.75
4.0	0.2306	3.52	3.28	2.724	-0.011	1.064	0.913	0.82	1.557	1.52
4.0	0.3164	3.73	3.18	2.044	0.015	0.738	0.824	0.66	1.476	1.41
4.0	0.4680	3.54	2.48	1.702	0.039	0.694	0.628	0.54	1.132	1.10

$$x = \frac{E}{\varepsilon C_1}\left(\frac{y_1}{E}\sqrt{1-\frac{y_1}{E}} - \frac{y}{E}\sqrt{1-\frac{y}{E}}\right) \quad \ldots\ldots\ldots\ldots (2.8a)$$

At the end of the rack $x = \ell$ and $y = y_2$; thus Eq. (2.8a) can be written for the coefficient of discharge, C_1, as follows:

$$C_1 = \frac{E}{\varepsilon \ell}\left[\frac{y_1}{E}\sqrt{1-\frac{y_1}{E}} - \frac{y_2}{E}\sqrt{1-\frac{y_2}{E}}\right] \quad \ldots\ldots\ldots\ldots (3.9)$$

C_1 is computed from the known values of y_1, y_2, ε, and the results are summarized in Table 4.

The relationship between the coefficient of discharge, C_1, and the Froude number, F_o, is depicted in Fig. 6. From the chart, it is observed that the coefficient of discharge depends upon the state of approach flow, whether subcritical or supercritical, and on the open area ratio. When the approach flow is supercritical, the coefficient of discharge varies considerably with the area factor. It decreases as the approach Froude number is increased. The coefficient of discharge is larger for subcritical flow than for supercritical case. In supercritical flow, the velocity is high and the flow has a tendency to jump over the rack because of the momentum. The flow diverted through the rack is therefore less than for subcritical case. The value of the coefficient of discharge therefore decreases as the Froude number is increased. The coefficient of discharge decreases as the open area increases. This is believed to be due to a flow acceleration resulting from the open area, thereby increasing F_o. Consequently, the coefficient of discharge, C_1, would decrease as the open area ratio increases.

TABLE 4

CALCULATION OF COEFFICIENT OF DISCHARGE C_1 FOR RACKS WITH SLITS

Area Factor ε	$q_1 = \frac{Q_1}{B}$	$q_3 = \frac{Q_3}{B}$	y_1	y_2	C_1	F_o
0.1445	817.44	207.60	7.41	4.58	0.348	1.30
	723.39	196.87	6.60	4.03	0.341	1.37
	638.41	167.22	5.64	3.65	0.294	1.37
	450.59	152.96	4.84	2.61	0.309	1.36
	334.56	126.78	3.84	1.96	0.281	1.43
	411.46	123.50	3.88	2.42	0.247	1.73
	525.83	111.59	3.70	2.80	0.183	2.38
	634.12	97.83	3.68	3.05	0.139	2.89
	754.73	86.57	3.84	3.36	0.110	3.22
	830.91	82.42	3.89	3.47	0.098	3.48
0.2911	821.35	364.14	7.14	3.15	0.299	1.38
	729.14	339.32	6.33	2.74	0.287	1.47
	582.43	295.01	5.39	2.14	0.267	1.50
	451.64	254.50	4.42	1.56	0.249	1.56
	341.39	217.63	3.74	1.06	0.236	1.52

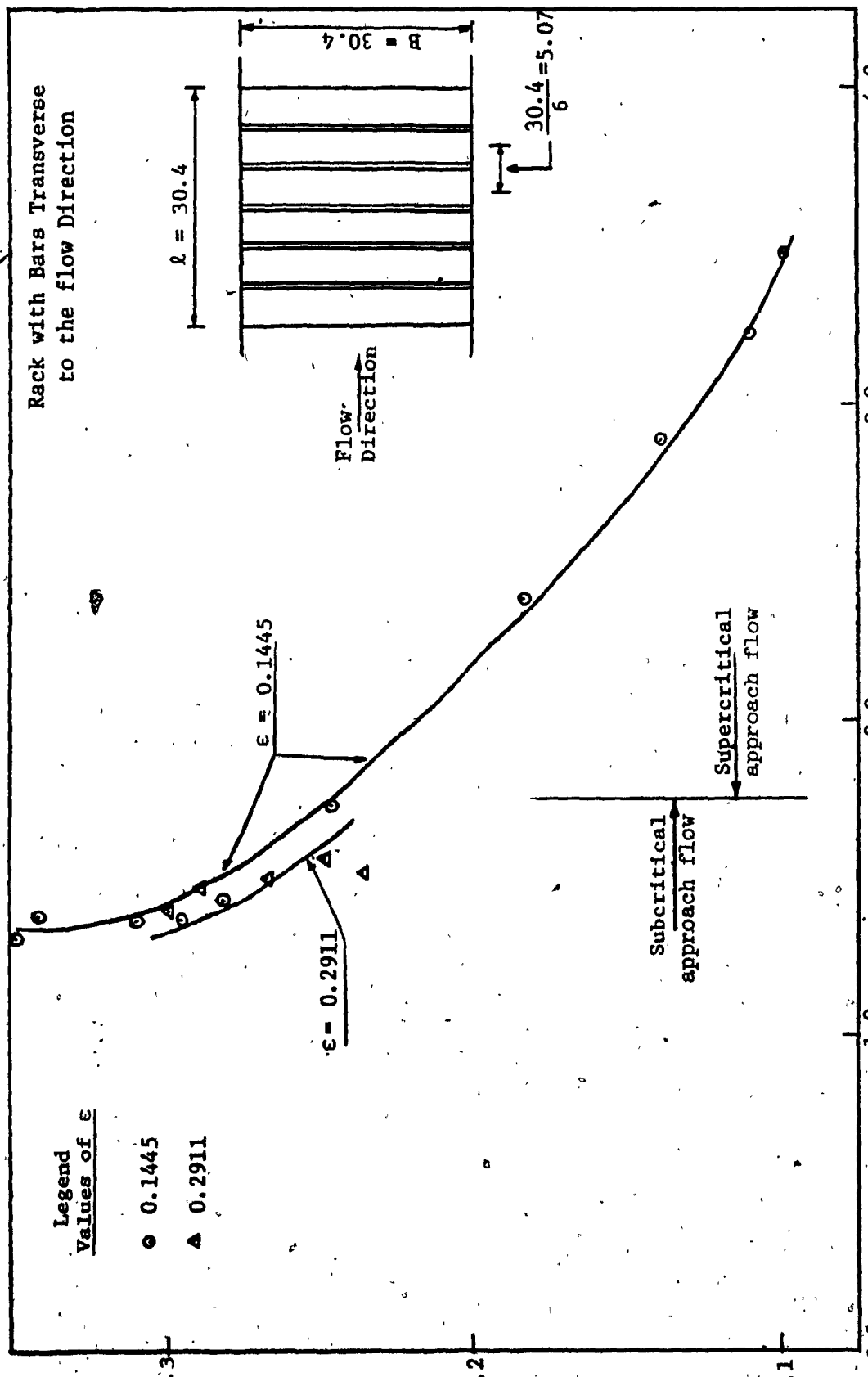

Fig. 6 — Variation of C_1 with F_o and ε.

3.3.2 Rack with Orifices

The equation proposed by Mostkow for flow profile over racks with orifices is:

$$x = \frac{E}{\varepsilon C_2}\left[\frac{1}{2}\cos^{-1}\sqrt{\frac{y}{E}} - \frac{3}{2}\sqrt{\frac{y}{E}\left(1-\frac{y}{E}\right)} - \frac{1}{2}\cos^{-1}\sqrt{\frac{y_1}{E}} + \frac{3}{2}\sqrt{\frac{y_1}{E}\left(1-\frac{y_1}{E}\right)}\right] \quad \ldots\ldots\ldots (2.8b)$$

At the end of the rack, $x = \ell$ and $y = y_2$, i.e.

$$C_2 = \frac{E}{\varepsilon \ell}\left[\frac{1}{2}\cos^{-1}\sqrt{\frac{y_2}{E}} - \frac{3}{2}\sqrt{\frac{y_2}{E}\left(1-\frac{y_2}{E}\right)} - \frac{1}{2}\cos^{-1}\sqrt{\frac{y_1}{E}} + \frac{3}{2}\sqrt{\frac{y_1}{E}\left(1-\frac{y_1}{E}\right)}\right] \quad \ldots\ldots\ldots (3.10)$$

Venkataraman's experimental data [15] of bottom racks with perforated screens with different area factors is analyzed and C_2 is computed. The results are summarized in Table 5. The variation of the coefficient of discharge, C_2, with the Froude number, F_o, of the incoming flow, for different values of the area factor, ε, is shown in Fig. 7. It is clear that the coefficient of discharge for a rack with a certain open area ratio, decreases as the approach Froude number increases. This is expected for the reasons already explained (pg. 27). For a certain F_o, the coefficient of discharge decreases as the opening area ratio is increased; this confirms Noseda's [11] observations (Art. 2.3).

The performance of racks with slits, Fig. 6, and racks with orifices, Fig. 7, with approximately the same opening area ratio are compared. It is found that the coefficient of discharge, C_1, for rack with parallel slits ($\varepsilon = 0.1445$), varies from 0.27 for subcritical flows to 0.10 for supercritical flows. The coefficient of discharge, C_2, for rack with orifices

TABLE 5

CALCULATION OF COEFFICIENT OF DISCHARGE C_2 WITH RACKS WITH ORIFICES

Area Factor-ε	$q_1 = \frac{Q_1}{B}$	$q_2 = \frac{Q_2}{B}$	y_1	y_2	C_2	F_o
0.0149	412.14	21.13	4.25	3.89	0.727	1.51
	526.53	19.20	3.93	3.75	0.727	2.17
	641.98	18.54	3.74	3.62	0.637	2.85
	749.35	18.13	3.99	3.88	0.679	3.02
	827.46	18.12	4.01	3.91	0.636	3.31
0.0595	814.64	130.37	8.06	5.56	0.883	1.14
	720.40	124.22	7.32	5.00	0.892	1.17
	572.60	110.39	6.19	4.12	0.865	1.19
	448.34	98.27	5.37	3.35	0.850	1.16
	335.50	89.15	4.48	2.54	0.864	1.14
	366.32	100.16	4.87	2.66	0.942	1.10
	524.18	68.95	3.81	3.21	0.646	2.27
	639.81	61.86	3.81	3.39	0.563	2.77
	756.05	55.63	3.93	3.61	0.511	3.12
	825.77	52.64	3.95	3.67	0.487	3.38
0.1339	812.63	238.87	7.45	4.26	0.785	1.28
	718.40	223.77	6.82	3.79	0.781	1.30
	568.53	199.26	5.73	2.99	0.768	1.33
	452.15	181.82	4.81	2.31	0.776	1.38
	338.19	154.11	4.01	1.71	0.743	1.35
	408.55	151.92	3.96	2.15	0.695	1.67
	527.81	141.30	3.74	2.59	0.622	2.35
	640.06	126.18	3.64	2.85	0.555	2.96
	758.27	113.96	3.82	3.20	0.469	3.26
	828.81	107.03	4.00	3.44	0.437	3.33

TABLE 5 (CONT'D)

Area Factor ϵ	$q_1 = \frac{Q_1}{B}$	$q_2 = \frac{Q_2}{B}$	y_1	y_2	C_2	F_0
0.238	816.16	328.94	7.04	3.40	0.654	1.40
	728.20	309.52	6.47	3.00	0.646	1.42
	576.20	273.87	5.41	2.30	0.637	1.48
	454.62	235.97	4.54	1.76	0.612	1.51
	335.92	196.41	3.68	1.21	0.588	1.53
0.238	414.43	195.20	3.80	1.74	0.527	1.80
	527.88	181.51	3.74	2.29	0.462	2.35
	641.32	164.95	3.65	2.63	0.406	3.00
	755.91	148.71	3.76	2.96	0.354	3.33
	823.32	130.12	4.05	3.35	0.296	3.25

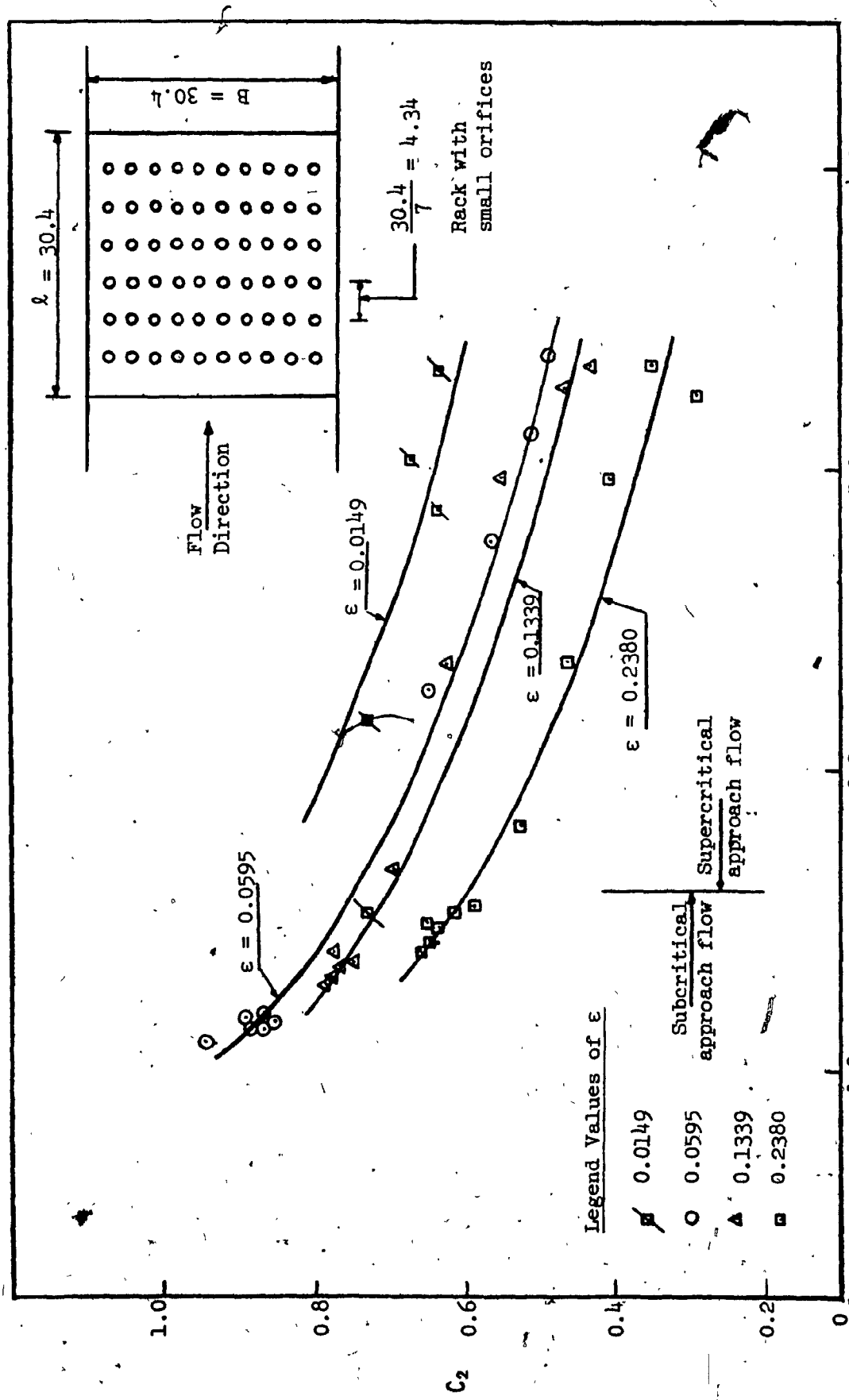

Fig. 7 — Variation of C_2 with F_o and ε.

(ϵ = 0.1339), varies from 0.72 for subcritical flow cases, to 0.45 for supercritical flows. In other words, racks with small orifices have greater discharging capacity than racks with transverse bars. This is contrary to the findings of Mostkow.

3.4 Surface Profile

The equations proposed by Mostkow [9] can now be employed to obtain the water surface profile over the racks. Methods of evaluating the coefficients of discharge C_1 or C_2 for racks with different configurations can be evaluated by methods already explained in Secs. 3.3.1 and 3.3.2.

Referring to Fig. 2, let y_1 be the depth of flow at the entrance to the rack and y_2 the depth at the end of the rack. The depths of flow along the rack can be predicted, when the specific energy E of the approach flow is known.

From the known upstream flow conditions (F_o and ϵ), the value of the coefficients of discharge (C_1 or C_2) can be obtained from Figs. 6 or 7 for the rack under study. Equations (3.9) and (3.10) can be rewritten as:

$$\delta\ell = \frac{E}{\epsilon C_1}\left[\frac{y_1}{E}\sqrt{1-\frac{y_1}{E}} - \frac{y}{E}\sqrt{1-\frac{y}{E}}\right] \qquad \ldots\ldots\ldots\ldots (3.11)$$

for a rack with parallel transverse bars, and

$$\delta\ell = \frac{E}{\epsilon C_2}\left[\frac{1}{2}\cos^{-1}\sqrt{\frac{y}{E}} - \frac{1}{2}\cos^{-1}\sqrt{\frac{y_1}{E}} + \frac{3}{2}\sqrt{\frac{y_1}{E}\left(1-\frac{y_1}{E}\right)} - \frac{3}{2}\sqrt{\frac{y}{E}\left(1-\frac{y}{E}\right)}\right]$$

$$\ldots\ldots\ldots\ldots (3.12)$$

where $\delta\ell$ = center-to-center spacing of the rack bars; Eqs. (3.11) and (3.12) can be written for the flow depth, y, as:

$$y^3 - Ey^2 + E\left(\delta \ell \epsilon C_1 - y_1 \sqrt{1 - \frac{y_1}{E}}\right)^2 = 0 \quad \ldots\ldots\ldots (3.13)$$

for a rack with parallel transverse bars, and

$$\frac{C_2 \epsilon \delta \ell}{E} + \frac{1}{2} \cos^{-1} \sqrt{\frac{y_1}{E}} - \frac{3}{2} \sqrt{\frac{y_1}{E}\left(1 - \frac{y_1}{E}\right)} = \frac{1}{2} \cos^{-1} \sqrt{\frac{y}{E}} - \frac{3}{2} \sqrt{\frac{y}{E}\left(1 - \frac{y}{E}\right)}$$

$\ldots\ldots\ldots (3.14)$

Equations (3.13) and (3.14) are solved by standard methods for the depths of flow at the center between the slits or row of orifices. These values are summarized in Tables 6 and 7, and are represented in Figs. 8 and 9, along with the experimental profiles.

The agreement between the profiles based on Mostkow's equations and the measured profiles appear to be satisfactory.

TABLE 6

CALCULATION OF WATER SURFACE PROFILE OVER RACK WITH PARALLEL BARS

	$\Delta\ell$	ϵ	C_1	y_1	y From Eq.	y From Exp.
I	10.13	0.1445	0.29	7.41	6.21	6.59
	15.20	"	"	"	5.74	5.93
	20.27	"	"	"	5.32	5.61
	25.33	"	"	"	4.94	5.38
II	10.13	0.1445	0.284	6.60	5.54	6.13
	15.20	"	"	"	5.11	5.39
	20.27	"	"	"	4.72	5.01
	25.33	"	"	"	4.37	4.68
III	10.13	0.1445	0.245	5.64	4.88	4.59
	15.20	"	"	"	4.54	4.45
	20.27	"	"	"	4.23	4.05
	25.33	"	"	"	3.93	3.89
IV	10.13	0.1445	0.258	4.84	3.90	4.02
	15.20	"	"	"	3.53	3.51
	20.27	"	"	"	3.20	3.16
	25.33	"	"	"	2.90	2.99
V	10.13	0.1445	0.234	3.84	3.06	3.25
	15.20	"	"	"	2.75	2.66
	20.27	"	"	"	2.47	2.39
	25.33	"	"	"	2.21	2.25

TABLE 7

CALCULATION OF WATER SURFACE PROFILE OVER RACK WITH ORIFICES

	$\Delta\ell$	ϵ	C_2	y_1	X	K	y From Eq.	y From Exp.
	4.34	0.1339	0.785	7.45	0.345	46.29	6.46	6.79
	8.69	"	"	"	0.311	49.29	5.75	6.33
I	13.03	"	"	"	0.278	51.80	5.17	5.60
	17.37	"	"	"	0.244	53.90	4.69	5.27
	21.71	"	"	"	0.210	55.80	4.27	4.85
	4.34	0.1339	0.781	6.82	0.342	46.65	5.88	6.24
	8.69	"	"	"	0.305	49.80	5.20	5.45
II	13.03	"	"	"	0.269	52.35	4.66	5.02
	17.37	"	"	"	0.232	54.55	4.20	4.58
	21.71	"	"	"	0.196	56.55	3.79	4.35
	4.34	0.1339	0.768	5.73	0.331	47.69	4.87	5.10
	8.69	"	"	"	0.289	50.97	4.26	4.42
III	13.03	"	"	"	0.247	53.68	3.77	4.00
	17.37	"	"	"	0.206	56.05	3.35	3.66
	21.71	"	"	"	0.164	58.18	2.99	3.44
	4.34	0.1339	0.776	4.81	0.317	48.87	4.03	4.24
	8.69	"	"	"	0.268	52.39	3.47	3.56
IV	13.03	"	"	"	0.220	55.27	3.03	3.16
	17.37	"	"	"	0.171	57.85	2.64	2.87
	21.71	"	"	"	0.123	60.13	2.31	2.76
	4.34	0.1339	0.743	4.01	0.313	49.21	3.26	3.32
	8.69	"	"	"	0.256	53.16	2.75	2.76
V	13.03	"	"	"	0.199	56.39	2.34	2.38
	17.37	"	"	"	0.143	59.22	2.00	2.10
	21.71	"	"	"	0.086	61.76	1.71	1.92

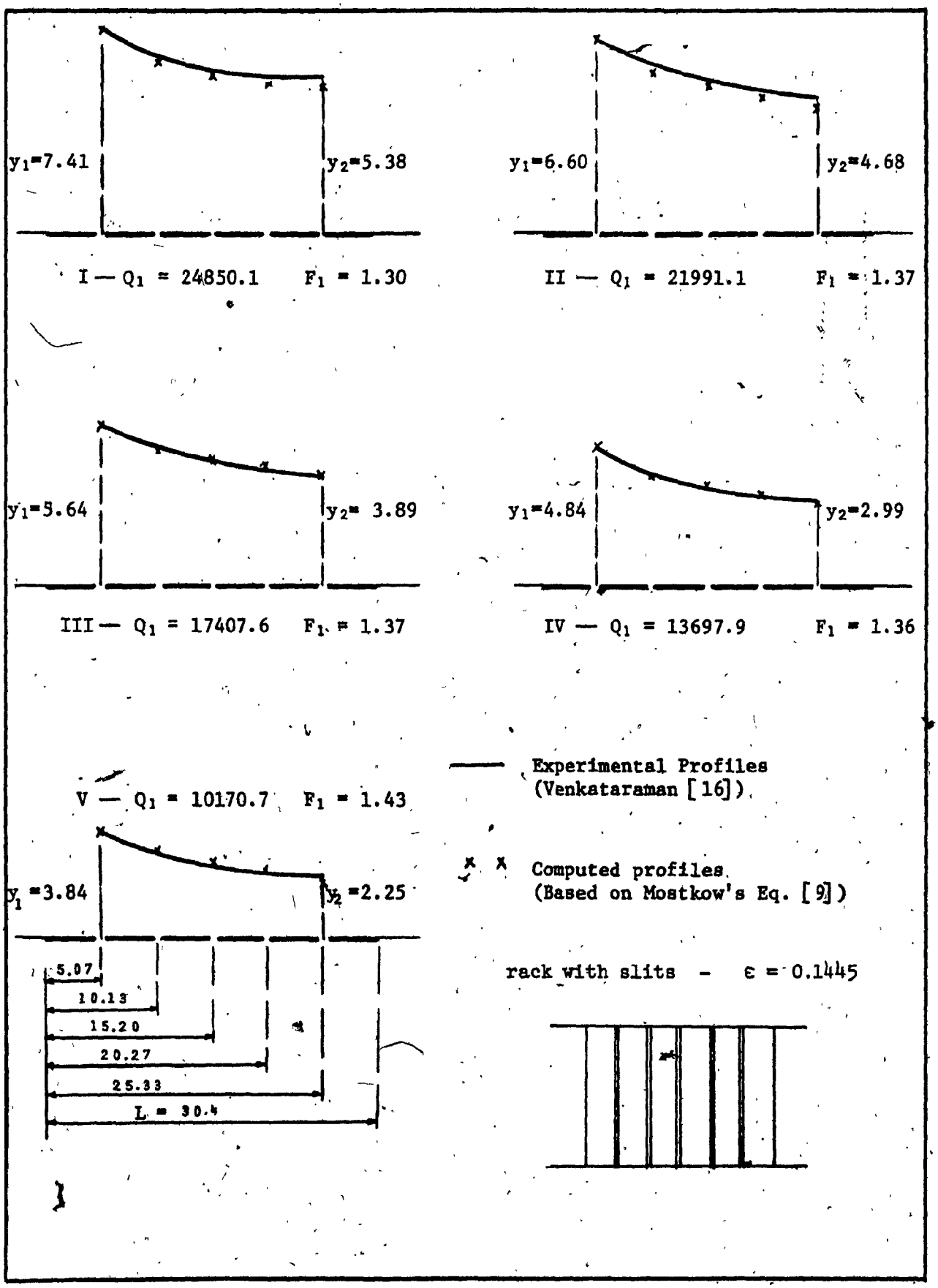

Fig. 8 — Flow profile over racks with slits.

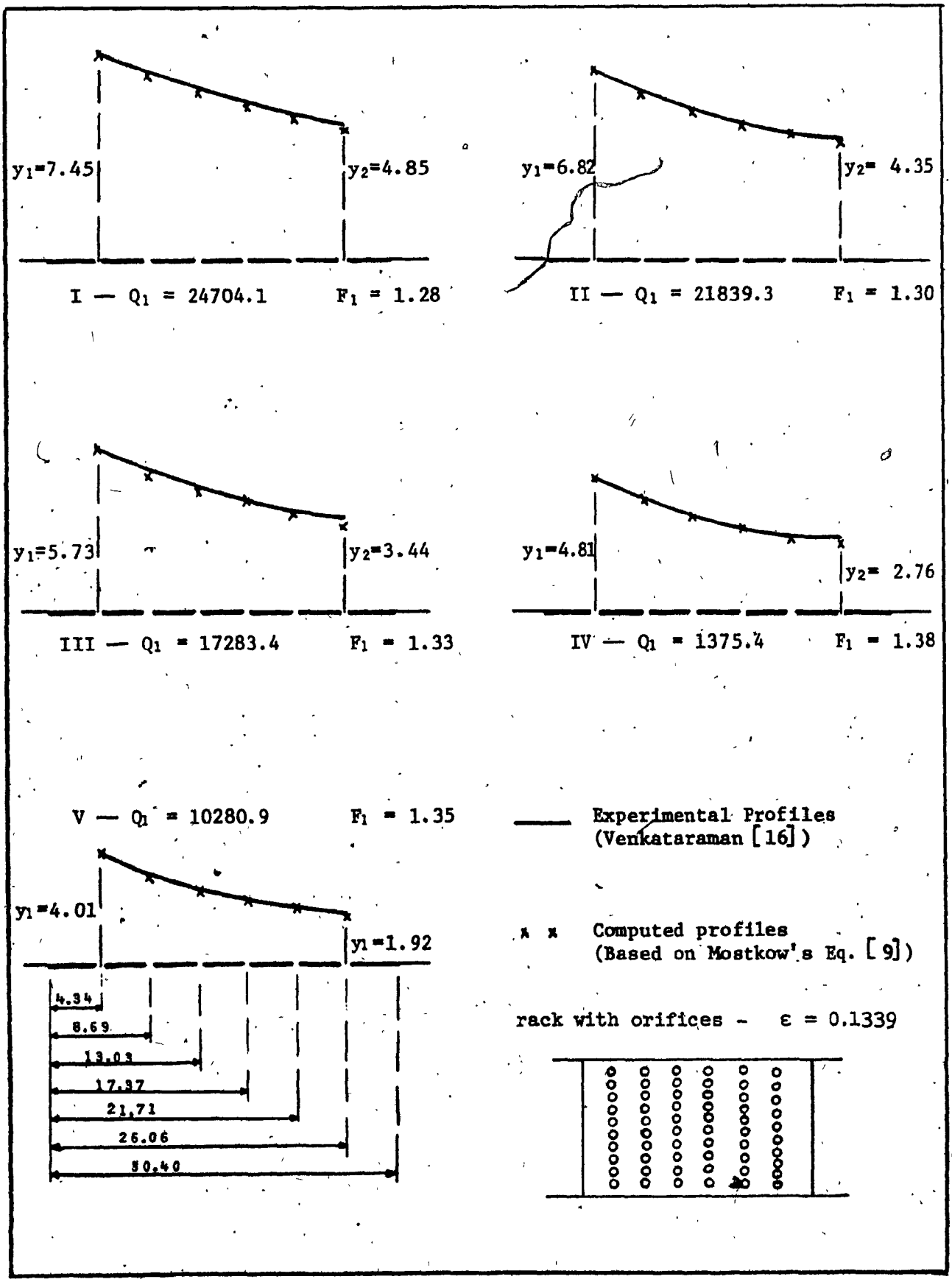

Fig. 9 — Flow profile over racks with orifices.

CHAPTER 4

CONCLUSIONS AND RECOMMENDATIONS

4.1 CONCLUSIONS

From the study presented, the following main conclusions are drawn:

1. The expression obtained for Y_o/ℓ in terms of the approach Froude number and the performance factor, Eq. (3.7), by resolving the momentum equation normal to the direction of flow, shows good agreement with the experimental data for supercritical flow cases.

2. The study reveals that for racks with small orifices, the coefficient of discharge, C_2, decreases as the approach Froude number increases. Also, for a certain Froude number, C_2 decreases as the opening ratio increases.

3. Water surface profiles predicted by Mostkow's equations for racks with narrow transverse slits and for racks with small orifices reasonably conform to the measured profiles.

4.2 RECOMMENDATIONS

This study gives rise to a few interesting points that warrant further investigations; these may be stated as follows:

1. From the review of the spatially varied flow equations, it is found that these equations need to be examined in view of the existing inconsistencies.

2. The investigation of flow in channels with bottom intakes indicates the need for a rationalized general theory for the design of bottom racks.

3. The analysis presented may be extended by considering the effects of the streamline curvature, the nonuniform velocity distribution and the bottom slope.

4. More data are needed to analyse the variation of the coefficient of discharge, C_1, for racks with parallel bars.

BIBLIOGRAPHY

1. AHMED, El-Khashab and K. V. SMITH. "Experimental investigation of flow over side weirs." Proc. A.S.C.E. Jol. of Hydr. Div., Vol. 102, No. HY4, pp. 1255-1268, 1976.

2. BOUVARD, M. "Debit d'une grille par en dessous." (Discharge passing through a bottom grid). La Houille Blanche, Grenoble, No. 2, May 1953.

3. CHOW, V.T. "Discussion of flood protection of canals by lateral spillways", by Harold Tults, Paper 1077, Proc. A.S.C.E., Journal Hydraulics Division, Vol. 83, No. HY2, pp. 47-49, April 1957.

4. _____. Open Channel Hydraulics. McGraw-Hill Book Co. Inc., New York, 1959.

5. _____. "Spatially varied flow equations". Journal, Water Resources Research, Vol. 5, No. 5, pp. 1124-1128, Oct. 1969.

6. DAGAN, G. (Drimmer). "Notes sur le calcul hydraulique des grilles (par-dessous)." (Note on the hydraulic design of bottom-type intake screens). La Houille Blanche, Grenoble, No. 1, Jan. 1963.

7. de MARCHI, G. "Saggio di teoria del funzionamento degli stramazzi laterali. (Essay of the performance of lateral weirs). L'Energia elettrica, Milano, Vol. 11, No. 11, pp. 849-860, Nov. 1934; reprinted as Istituto di Idraulica e costruzioni Idrauliche, Milano, Memorie e studi No. 11, 1934.

8. HINDS, J. "Side channel spillway: hydraulic theory, economic factors, and experimental determination of losses." Trans. A.S.C.E. Vol. 89, 1926, pp. 881-927.

9. MOSTKOW, M.A. "Sur le calcul des grilles de prise d'eau." (Theoretical study of bottom type water intake). La Houille Blanche, Grenoble, No. 4, Sept. 1957.

10. NIMMO, H.R. "Side spillways for regulating diversion canals." Trans. A.S.C.E. Vol. 92, pp. 1561-1584, 1928.

11. NOSEDA, G. "Operation and design of bottom intake racks." Proceedings of the 6th General Meeting, International Association of Hydraulic Research, The Hague, 1955, Vol. 3, p. c.17.I.

12. ORTH, J., E. CHARDONNET and G. MEYNARDI. "Etude des grilles pour prises d'eau du type en dessous." (Study of bottom type water intake grids). La Houille Blanche, Grenoble, No. 3, June 1954.

13. VENKATARAMAN, P. "Divided flow in channels with bottom openings." Journal of the Hyd. Div., A.S.C.E., Vol. 103, No. HY2, Proc. Paper 12711, Feb. 1977, pp. 190-194.

14. ————. "Discharge characteristics of an idealized bottom intake." Journal of the Institution of Engineers, (India), Vol. 58, Sept.-Nov. 1977.

15. ————. "Some studies on steady spatially varied flow in open channels with decreasing discharge." Thesis presented to Sri Venkateswara University, at Tirupati, Andhra Pradesh, India, in 1977, in partial fulfillment of the requirements for the degree of Doctor of Philosophy.

16. VENKATARAMAN, P., M.S. NASSER, and A.S. RAMAMURTHY. "Flow behaviour in power channels with bottom diversion works." Paper accepted for presentation at the 18th Congress of IAHR to be held at Cagliari, Italy, in Sept. 1979.

17. B.C. YEN and H.G. WENZEL. "Dynamic equations for steady spatially varied flow." Proc. A.S.C.E., Vol. 96, No. HY3, March 1970.

APPENDIX I

EXPERIMENTAL SET-UP AND MEASURING TECHNIQUES

General Remarks

The analysis presented in the study is based on the data made available to the writer from Ref. 15. This Appendix presents the details of experimental set-up, range of variables tested and their accuracies as given in Ref. 15.

Experiments were conducted in a glass-walled, rectangular, horizontal flume of 12.0 m length and 30 cm width (B) (Fig. 10). Facilities existed to introduce a slit with adjustable length (ℓ), at a distance of 5.0 ms from the entrance section. All discharges were measured with the aid of right angled V-notches. The head over the notch was measured with the aid of hook gauges (L.C. = 0.001 mms), while the elevations of the water surface were measured using a pointer gauge (L.C. = 0.001 mms).

The measured discharges are estimated to have been within an accuracy of 2% at low flows and 3% at high flows. The range of discharges varied from 15 to 60 litres per second in the case of slots and up to 25 litres per second in the tests involving bottom racks.

Experiments were first conducted on different sizes of rectangular sharp-edged slots formed at the bed of a channel and spanning its entire width. Racks with bars arranged transverse to the flow direction and racks with perforations were then tested and their effects on the flow

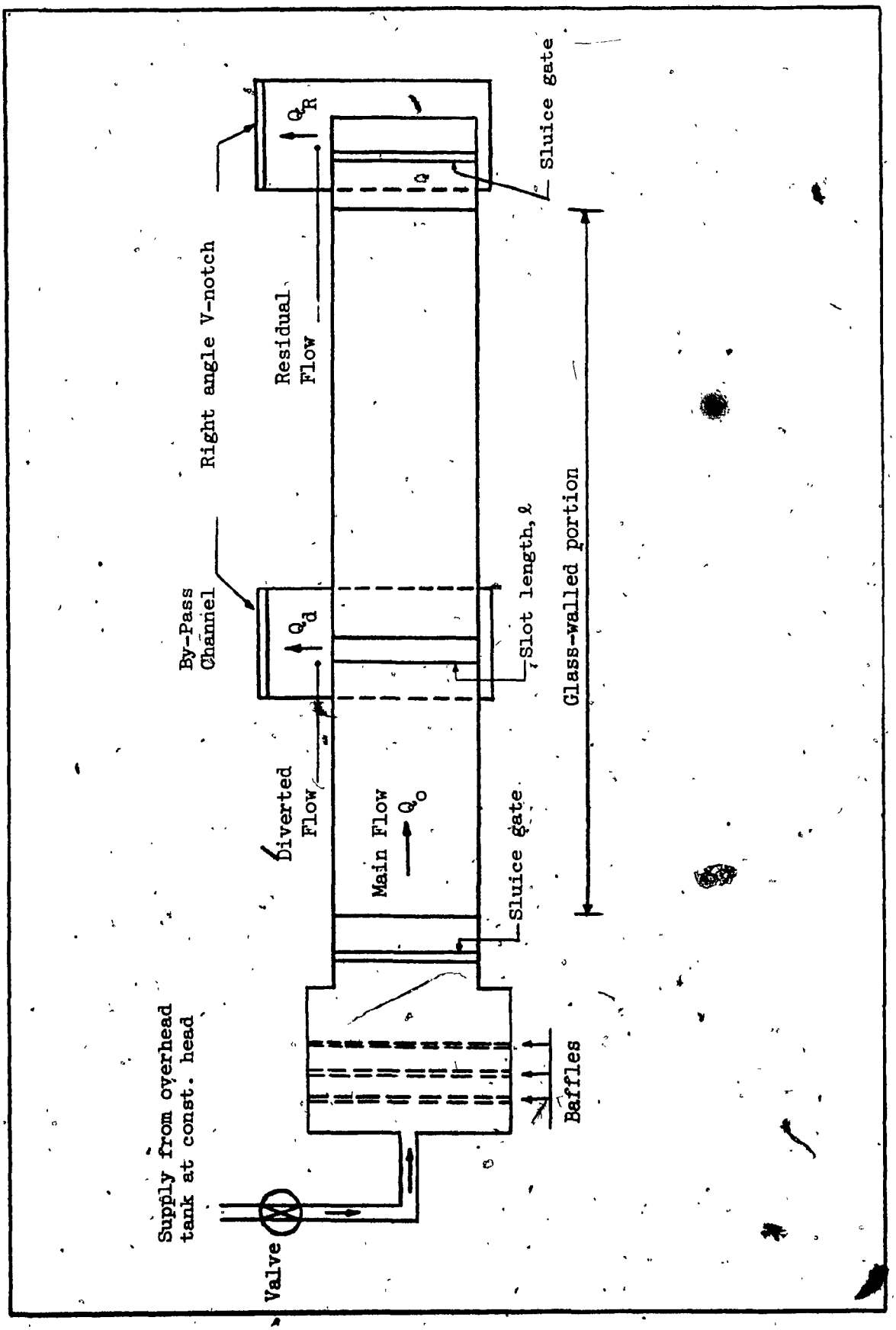

Fig. 10 — Experimental Set-up.

behaviour studied.

In the case of experiments on supercritical flow, the Froude number of the approach flow was varied with the aid of an upstream gate.